type in the alkyne and thus tend to weaken the Nb–Nb bonding. Compared with the M–M bonding in $W_2Cl_4(NMe_2)_2(\mu$-$MeCCMe)(py)_2$, the occupation of the $15a_1$ orbital in the W complex (see Figure 6b,c) makes the bonding interaction between the W atoms stronger than that between the Ta atoms in $Ta_2Cl_6(Me_3CCCCMe_3)(THF)_2$. Taken together with the consideration of the relative size of the bridging N and Cl atoms in the two molecules, this provides a good explanation for the W–W distance (2.436 Å) being shorter than the Ta–Ta distance.

To summarize, this work fully supports the previous proposal[3] that a large deviation of a bridging alkyne from perpendicularity (to the M–M bond) is due to a small HOMO–LUMO gap (with the perpendicular geometry) from which a second-order Jahn–Teller effect arises. It further shows that a similar explanation applies in a different case and, importantly, that the converse is true; namely, in a case where no significant deviation occurs, the calculated HOMO–LUMO gap is large. Thus the conceptual approach embodied by this and the previous[3] work appears to have general validity.

Acknowledgment. We thank the National Science Foundation for support.

Contribution from the Laboratory for Molecular Structure and Bonding, Department of Chemistry, Texas A&M University, College Station, Texas 77843

A New Type of Metal–Olefin Complex. Synthesis and Characterization of Four Compounds That Contain an Ethylene Bridge Perpendicularly Bisecting a Metal–Metal Axis

F. Albert Cotton* and Piotr A. Kibala

Received November 7, 1989

The edge-sharing bioctahedral dimers $M_2X_6(PR_3)_4$ (M = Zr, Hf; X = Cl, Br; R = Et) react readily with 1,2-dichloroethane and ethylene to yield a novel type of metal–olefin complex, $M_2X_6(PR_3)_4(CH_2CH_2)$. The characteristic feature of these complexes is a symmetrical olefin bridge, in which the olefin plane is perpendicular to the metal–metal axis, with the midpoint of the olefin coinciding with the midpoint of the metal–metal axis. Each compound was characterized by single-crystal X-ray diffraction studies. $Zr_2Cl_6(PEt_3)_4(CH_2CH_2)$ (**1**): orthorhombic space group *Pbca*; a = 12.444 (3) Å, b = 15.878 (2) Å, c = 21.394 (4) Å, V = 4227 (2) Å^3, and d_{calc} = 1.408 g/cm^3 for Z = 4. The structure was refined to R = 0.0628 and R_w = 0.0760 for 1021 reflections having $I > 3\sigma(I)$. $Zr_2Br_6(PEt_3)_4(CH_2CH_2)$ (**2**): monoclinic space group $P2_1/n$; a = 11.538 (3) Å, b = 15.063 (5) Å, c = 13.010 (4) Å, β = 108.41 (2)°, V = 2145 (2) Å^3, and d_{calc} = 1.800 g/cm^3 for Z = 2. The structure was refined to R = 0.0543 and R_w = 0.0697 for 1109 reflections having $I > 3\sigma(I)$. $Hf_2Cl_6(PEt_3)_4(CH_2CH_2)$ (**3**): orthorhombic space group *Pbca*; a = 12.393 (3) Å, b = 15.922 (6) Å, c = 21.339 (6) Å, V = 4211 (4) Å^3, and d_{calc} = 1.688 g/cm^3 for Z = 4. The structure was refined to R = 0.0318 and R_w = 0.0480 for 1841 reflections having $I > 3\sigma(I)$. $Hf_2Br_6(PEt_3)_4(CH_2CH_2)$ (**4**): monoclinic space group $P2_1/n$; a = 11.482 (2) Å, b = 15.093 (1) Å, c = 12.979 (2) Å, β = 108.14 (1)°, V = 2137 (1) Å^3, and d_{calc} = 2.034 g/cm^3 for Z = 2. The structure was refined to R = 0.0393 and R_w = 0.0531 for 1109 reflections with $I > 3\sigma(I)$. Molecular orbital calculations on $Zr_2Cl_6(PH_3)_4(CH_2CH_2)$ by the Fenske–Hall method have been carried out to elucidate the bonding in the $M_2(\mu$-η^4-olefin) unit. The calculations show a HOMO resulting from an overlap between suitable dπ orbitals on the metal atoms with the π^* orbital of CH_2CH_2.

Introduction

In recent years dinuclear transition-metal complexes containing saturated hydrocarbon bridges between metal centers received considerable attention in hope of gaining some insight into catalytic processes occurring on metal surfaces.[1-3] These compounds are viewed as the first step toward understanding the relationship between the chemistry of soluble organometallic compounds and the chemistry of solid metal catalysts. In fact, it is hoped that a smooth transition from the chemistry of mononuclear compounds to dinuclear compounds to metal clusters to metal surfaces will take place.

Dinuclear transition-metal complexes with saturated hydrocarbon groups bridging between the metal centers fall into two major structural categories: dinuclear compounds without a metal–metal bond, I, and dinuclear compounds with a metal–metal

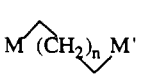

$n \geq 1$

I

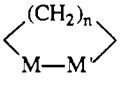

II

bond, II. These compounds may be heteronuclear (M ≠ M') or homonuclear (M = M') with respect to the metal atoms. In either of the two categories, metal–carbon bonds are of the σ type and the compounds might be viewed as alkanes with heteroatoms: α,ω-dimetallaalkanes (I) and dimetallacycloalkanes (II).

In 1987 we published a preliminary report[4] on the synthesis of a new type of compound with a hydrocarbon bridge, $Zr_2X_6(PEt_3)_4(CH_2CH_2)$ (X = Cl, Br), that does not fall into either of the above categories. The characteristic feature of these molecules is an ethylene bridge that forms a perpendicular bisector of the metal–metal axis. These compounds are the first examples of another category of hydrocarbon-bridged dinuclear metal complexes, III, shown schematically.

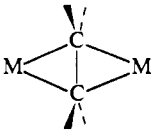

III

Since publishing our report we have synthesized several more of these new species. This paper presents a full account of this work including syntheses, structures, and a molecular orbital description of four $M_2X_6(PR_3)_4(CH_2CH_2)$ compounds (M = Zr, Hf; X = Cl, Br; R = Et).

* To whom correspondence should be addressed.

(1) Casey, C. P.; Audett, J. D. *Chem. Rev.* **1986**, *86*, 339.
(2) Moss, J. R.; Scott, L. G. *Coord. Chem. Rev.* **1984**, *60*, 171.
(3) Holton, J.; Lappert, M. F.; Pearce, R.; Yarrow, P. I. *Chem. Rev.* **1983**, *83*, 135.
(4) Cotton, F. A.; Kibala, P. A. *Polyhedron* **1987**, *6*, 645.

0020-1669/90/1329-3192$02.50/0

Table I. Crystal Data for $Zr_2Cl_6(PEt_3)_4(CH_2CH_2)$ (**1**), $Zr_2Br_6(PEt_3)_4(CH_2CH_2)$ (**2**), $Hf_2Cl_6(PEt_3)_4(CH_2CH_2)$ (**3**), and $Hf_2Br_6(PEt_3)_4(CH_2CH_2)$ (**4**)

	1	**2**	**3**	**4**
formula	$C_{26}H_{64}Cl_6P_4Zr_2$	$C_{26}H_{64}Br_6P_4Zr_2$	$C_{26}H_{64}Cl_6P_4Hf_2$	$C_{26}H_{64}Br_6P_4Hf_2$
fw	895.85	1162.59	1070.39	1309.1
space group	*Pbca*	$P2_1/n$	*Pbca*	$P2_1/n$
a, Å	12.444 (3)	11.538 (3)	12.393 (3)	11.482 (2)
b, Å	15.878 (2)	15.063 (5)	15.922 (6)	15.093 (1)
c, Å	21.394 (4)	13.010 (4)	21.339 (6)	12.979 (2)
α, deg	90.0	90.0	90.0	90.0
β, deg	90.0	108.41 (2)	90.0	108.14 (1)
γ, deg	90.0	90.0	90.0	90.0
V, Å^3	4227 (2)	2145 (2)	4211 (4)	2137 (1)
Z	4	2	4	2
d_{calc}, g/cm^3	1.408	1.800	1.688	2.034
T, °C	4	4	20	21
λ(Mo Kα), Å	0.71073	0.71073	0.71073	0.71073
μ(Mo Kα), cm^{-1}	10.34	61.78	54.36	105.315
transm factors: max, min	0.999, 0.992	0.998, 0.923	0.998, 0.614	0.999, 0.551
R^a	0.0628	0.0543	0.0318	0.0393
$R_w{}^b$	0.0760	0.0697	0.0480	0.0531

$^a R = \sum||F_o| - |F_c||/\sum|F_o|$. $^b R_w = [\sum w(|F_o| - |F_c|)^2/\sum w|F_o|^2]^{1/2}$; $w = 1/\sigma^2(|F_o|)$.

Experimental Section

All manipulations were carried out under an argon atmosphere by using standard vacuum-line and Schlenk techniques. The solvents were freshly distilled under nitrogen from the appropriate drying agent. $ZrCl_4$ and $HfCl_4$ were purchased from Strem, $ZrBr_4$ and $HfBr_4$ were obtained from Cerac, and PEt_3 and CH_2CH_2 were obtained from Aldrich. They were used as received.

Synthesis of $Zr_2Cl_6(PEt_3)_4(CH_2CH_2)$ (1). Method A. $ZrCl_4$ (1.00 g, 4.3 mmol), PEt_3 (1.30 mL, 8.8 mmol), and 2.2 M Na/Hg (2.00 mL, 4.4 mmol) were stirred vigorously in 20 mL of toluene for 24 h. The green solution of $Zr_2Cl_6(PEt_3)_4$[5] was filtered through Celite (2 cm) into a round-bottom flask. Additional $Zr_2Cl_6(PEt_3)_4$ was recovered by washing the solid residue with 40 mL of toluene. A 35-mL aliquot of 1,2-dichloroethane was added to the combined solutions of $Zr_2Cl_6(PEt_3)_4$. An immediate color change from green to orange was observed. The flask was placed in a freezer (−20 °C) for 2 weeks. After that time a crop of orange plates was separated from the solution via filtration. The isolated yield was 0.24 g (12%).

Method B. $Zr_2Cl_6(PEt_3)_4$ (0.5 g, 0.6 mmol) was dissolved in toluene (20 mL). A slow stream of ethylene was passed through the solution for 5 min. Within seconds the solution changed its color from green to brown to orange and crystalline material started precipitating to the bottom of the reaction flask. The flask was placed in a freezer (−20 °C) for 1 week. After that time the crystalline orange product was separated from the solution via filtration in approximately 100% yield. A single-crystal X-ray diffraction study showed this material to be identical with the product obtained by method A.

Synthesis of $Zr_2Br_6(PEt_3)_4(CH_2CH_2)$ (2). This material was synthesized by a slight modification of method A used in the preparation of $Zr_2Cl_6(PEt_3)_4(CH_2CH_2)$ (**1**). $ZrBr_4$ (1.79 g, 4.4 mmol), PEt_3 (1.30 mL, 8.8 mmol), and 2.2 M Na/Hg (2.00 mL, 4.4 mmol) were stirred vigorously in 20 mL of toluene for 24 h. 1,2-Dichloroethane (35 mL) was added to the green suspension of the presumed $Zr_2Br_6(PEt_3)_4$ species. An immediate reaction took place, as evidenced by dissolution of the green suspension to form an orange solution. The solution was filtered through Celite (2 cm) into another flask and was placed in a freezer (−20 °C) for 2 weeks. After that time a crop of red, X-ray-quality crystals was separated from the solution via filtration. The yield was 0.74 g (29%).

Synthesis of $Hf_2Cl_6(PEt_3)_4(CH_2CH_2)$ (3) and $Hf_2Br_6(PEt_3)_4(CH_2CH_2)$ (4). Yellow, X-ray-quality crystals of **3** and **4** were prepared by reacting toluene solutions of the presumed $Hf_2X_6(PEt_3)_4$ (X = Cl, Br) species with either 1,2-dichloroethane or ethylene and placing the reaction flasks in a freezer (−20 °C) for 1–2 weeks. In all cases the yields were very low (<10%). The toluene solutions of the presumed $Hf_2X_6(PEt_3)_4$ species were obtained by Na/Hg reduction of appropriate hafnium(IV) halide in the presence of PEt_3 in toluene. The solutions were separated from the solid residues via filtration through Celite (2 cm).

X-ray Crystallography

All crystals in this study were mounted and sealed with epoxy glue in thin-walled capillaries filled with degassed mineral oil to prevent decomposition in the air. Axial lengths and Laue class were confirmed with oscillation photographs. The general procedures were routine to this laboratory and have already been described.[6] Lorentz, polarization, and empirical absorption corrections were applied to the data. The positions of heavy atoms were deduced from the Patterson maps. Additional least-squares cycles and difference Fourier maps revealed the positions of the remaining non-hydrogen atoms. All atoms were refined anisotropically. No disorder or other nonroutine problems arose. A summary of crystal and refinement data is presented in Table I. The atomic positional parameters for $Zr_2Cl_6(PEt_3)_4(CH_2CH_2)$ (**1**), $Zr_2Br_6(PEt_3)_4(CH_2CH_2)$ (**2**), $Hf_2Cl_6(PEt_3)_4(CH_2CH_2)$ (**3**), and $Hf_2Br_6(PEt_3)_4(CH_2CH_2)$ (**4**), are given in Tables II–V, respectively.

Table II. Positional and Equivalent Isotropic Displacement Parameters and Their Estimated Standard Deviations for $Zr_2Cl_6(PEt_3)_4(CH_2CH_2)$[a]

atom	x	y	z	B_{eqv}, Å^2
Zr	0.0137 (1)	0.0611 (1)	0.09607 (8)	3.35 (3)
Cl(1)	−0.1163 (5)	0.1616 (3)	0.0559 (3)	6.1 (1)
Cl(2)	0.1412 (4)	−0.0466 (3)	0.1275 (2)	4.9 (1)
Cl(3)	0.0151 (5)	0.1413 (3)	0.1951 (2)	6.2 (1)
P(1)	0.1949 (4)	0.1617 (3)	0.0823 (2)	3.8 (1)
P(2)	−0.1341 (5)	−0.0303 (4)	0.1671 (3)	5.3 (1)
C(10)	0.053 (2)	0.029 (1)	−0.0122 (8)	4.2 (5)
C(11)	0.275 (2)	0.163 (1)	0.1573 (8)	5.7 (6)
C(12)	0.384 (2)	0.215 (1)	0.154 (1)	6.6 (6)
C(13)	0.296 (2)	0.138 (1)	0.0222 (8)	5.9 (6)
C(14)	0.356 (2)	0.053 (1)	0.031 (1)	7.4 (6)
C(15)	0.159 (2)	0.277 (1)	0.070 (1)	7.8 (7)
C(16)	0.115 (2)	0.290 (1)	0.008 (1)	9.8 (8)
C(21)	−0.262 (3)	0.036 (2)	0.185 (1)	13 (1)
C(22)	−0.315 (2)	0.028 (2)	0.133 (1)	15 (1)
C(23)	−0.154 (2)	−0.141 (1)	0.145 (1)	8.9 (7)
C(24)	−0.224 (3)	−0.193 (2)	0.186 (1)	13 (1)
C(25)	−0.111 (3)	−0.038 (2)	0.253 (1)	12 (1)
C(26)	−0.037 (3)	−0.090 (2)	0.272 (1)	16 (1)

[a] The equivalent isotropic displacement parameter, B_{eqv}, is calculated as $^1/_3[a^2a^{*2}B_{11} + b^2b^{*2}B_{22} + c^2c^{*2}B_{33} + 2ab(\cos\gamma)a^*b^*B_{12} + 2ac(\cos\beta)a^*c^*B_{13} + 2bc(\cos\alpha)b^*c^*B_{23}]$.

Computational Procedures

The molecular orbital calculation[7] on a model compound $Zr_2Cl_6(PH_3)_4(CH_2CH_2)$ was carried out by the approximate nonempirical Fenske–Hall molecular orbital method.[8] Metal atom basis functions

(5) (a) Wengrovius, J. H.; Schrock, R. R.; Day, C. S. *Inorg. Chem.* **1981**, *20*, 1844. (b) Cotton, F. A.; Diebold, M. P.; Kibala, P. A. *Inorg. Chem.* **1988**, *27*, 799.

(6) (a) Bino, A.; Cotton, F. A.; Fanwick, P. E. *Inorg. Chem.* **1979**, *18*, 3558. (b) Cotton, F. A.; Frenz, B. A.; Deganello, G.; Shaver, A. J. *J. Organomet. Chem.* **1973**, *50*, 227. (c) North, A. C. T.; Phillips, D. C.; Mathews, F. S. *Acta Crystallogr., Sect. A.: Cryst. Phys., Diffr., Theor. Gen. Crystallogr.* **1968**, *A24*, 351. (d) Walker, N.; Stuart, D. *Acta Crystallogr., Sect. A.: Found. Crystallogr.* **1983**, *A39*, 158.

(7) The calculations were performed on the Microvax II computer at the Laboratory for Molecular Structure and Bonding, Department of Chemistry, Texas A&M University, College Station, TX 77843.

(8) Fenske, R. F.; Hall, M. B. *Inorg. Chem.* **1972**, *11*, 768.

Table III. Positional and Equivalent Isotropic Displacement Parameters and Their Estimated Standard Deviations for $Zr_2Br_6(PEt_3)_4(CH_2CH_2)$[a]

atom	x	y	z	B_{eqv}, Å^2
Zr	0.5368 (2)	−0.0013 (2)	0.3381 (2)	2.02 (4)
Br(1)	0.7087 (3)	0.1106 (2)	0.4322 (2)	4.58 (7)
Br(2)	0.3682 (2)	−0.1211 (2)	0.2713 (2)	4.04 (7)
Br(3)	0.6007 (3)	0.0189 (2)	0.1626 (2)	4.92 (7)
P(1)	0.3481 (6)	0.1062 (4)	0.2108 (4)	2.8 (2)
P(2)	0.6841 (6)	−0.1512 (4)	0.3607 (5)	3.2 (2)
C(10)	0.452 (2)	0.038 (1)	0.479 (1)	2.3 (5)
C(11)	0.279 (3)	0.061 (2)	0.072 (2)	4.7 (7)
C(12)	0.173 (2)	0.113 (2)	−0.001 (2)	5.7 (8)
C(13)	0.213 (2)	0.129 (2)	0.255 (2)	3.9 (6)
C(14)	0.132 (2)	0.045 (2)	0.254 (2)	5.3 (8)
C(15)	0.400 (2)	0.222 (1)	0.191 (2)	3.7 (6)
C(16)	0.441 (2)	0.273 (2)	0.296 (2)	4.8 (8)
C(21)	0.848 (2)	−0.132 (2)	0.440 (2)	6.4 (9)
C(22)	0.917 (2)	−0.076 (2)	0.384 (2)	6.4 (9)
C(23)	0.632 (2)	−0.241 (2)	0.434 (2)	4.7 (7)
C(24)	0.702 (3)	−0.330 (2)	0.442 (3)	8 (1)
C(25)	0.702 (2)	−0.203 (2)	0.237 (2)	4.1 (7)
C(26)	0.575 (2)	−0.238 (2)	0.156 (2)	5.4 (8)

[a] The equivalent isotropic displacement parameter, B_{eqv}, is calculated as $^1/_3[a^2a^{*2}B_{11} + b^2b^{*2}B_{22} + c^2c^{*2}B_{33} + 2ab(\cos\gamma)a^*b^*B_{12} + 2ac(\cos\beta)a^*c^*B_{13} + 2bc(\cos\alpha)b^*c^*B_{23}]$.

Table IV. Positional and Equivalent Isotropic Displacement Parameters and Their Estimated Standard Deviations for $Hf_2Cl_6(PEt_3)_4(CH_2CH_2)$[a]

atom	x	y	z	B_{eqv}, Å^2
Hf	0.01301 (3)	0.06068 (2)	0.09529 (2)	3.493 (8)
Cl(1)	−0.1154 (3)	0.1617 (2)	0.0557 (2)	6.16 (7)
Cl(2)	0.1407 (2)	−0.0449 (2)	0.1277 (1)	5.07 (6)
Cl(3)	0.0116 (3)	0.1407 (2)	0.1944 (2)	6.72 (8)
P(1)	0.1932 (2)	0.1615 (2)	0.0823 (1)	4.19 (6)
P(2)	−0.1353 (3)	−0.0300 (2)	0.1652 (2)	5.72 (8)
C(10)	0.0454 (9)	0.0255 (6)	−0.0117 (4)	4.0 (2)
C(11)	0.272 (1)	0.1663 (7)	0.1554 (6)	6.1 (3)
C(12)	0.380 (1)	0.2178 (8)	0.1516 (7)	8.2 (4)
C(13)	0.2937 (9)	0.1383 (7)	0.0231 (6)	5.8 (3)
C(14)	0.356 (1)	0.0519 (8)	0.0342 (7)	7.8 (4)
C(15)	0.158 (1)	0.2739 (7)	0.0693 (6)	7.3 (3)
C(16)	0.109 (1)	0.2922 (9)	0.0070 (8)	9.9 (5)
C(21)	−0.274 (2)	0.046 (1)	0.1806 (8)	18.0 (6)
C(22)	−0.308 (2)	0.017 (1)	0.1301 (9)	16.9 (6)
C(23)	−0.148 (1)	−0.1405 (7)	0.1415 (6)	8.8 (4)
C(24)	−0.225 (2)	−0.1940 (9)	0.1818 (9)	12.9 (6)
C(25)	−0.106 (2)	−0.0360 (8)	0.2516 (7)	12.2 (6)
C(26)	−0.042 (2)	−0.094 (2)	0.2721 (9)	17.9 (8)

[a] The equivalent isotropic displacement parameter, B_{eqv}, is calculated as $^1/_3[a^2a^{*2}B_{11} + b^2b^{*2}B_{22} + c^2c^{*2}B_{33} + 2ab(\cos\gamma)a^*b^*B_{12} + 2ac(\cos\beta)a^*c^*B_{13} + 2bc(\cos\alpha)b^*c^*B_{23}]$.

were taken from Richardson[9] and were augumented by 5s and 5p functions with exponents of 2.20 for zirconium.[10] Double-ζ basis sets of Clementi[11] were utilized for the main-group elements, phosphorus, chlorine, sulfur, and hydrogen. An exponent of 1.2 was used for the hydrogen atom. The atomic coordinates used in the calculation were taken from the crystal structure data for $Zr_2Cl_6(PEt_3)_4(CH_2CH_2)$ and were idealized to give the molecule D_{2h} symmetry. Atomic coordinates of the hydrogen atoms were calculated to fit the idealized geometry of the model. The coordinate system for $Zr_2Cl_6(PH_3)_4(CH_2CH_2)$ was chosen so that the origin was placed at the midpoint between zirconium and ethylene carbon atoms. The Z axis was located along the Zr–Zr vector, and the X axis along a vector drawn between the ethylene carbon atoms. For each atom a local right-hand coordinate system was chosen as follows: the z axis of the local system points toward either the origin or one of the zirconium atoms, whichever is the nearest, the y axis points toward the negative direction of the Z axis or toward the positive direction of Y axis of the molecular coordinate system, when the former is not possible, and the x axis is parallel to the XY plane of the molecular system.

(9) Richardson, J. W.; Blackman, M. J.; Ranochak, J. E. *J. Chem. Phys.* **1973**, *58*, 3010.
(10) Barber, M.; Connor, J. A.; Guest, M. F., Hall, M. B.; Hillier, I. H.; Meredith, W. N. E. *J. Chem. Soc., Faraday. Trans. 2* **1972**, *54*, 219.
(11) Tables of Atomic Functions, a supplement to a paper by E. Clementi; *IBM J. Res. Dev.* **1965**, *9*, 2.

Table V. Positional and Equivalent Isotropic Displacement Parameters and Their Estimated Standard Deviations for $Hf_2Br_6(PEt_3)_4(CH_2CH_2)$[a]

atom	x	y	z	B_{eqv}, Å^2
Hf	0.53483 (6)	−0.00223 (5)	0.33903 (5)	2.27 (1)
Br(1)	0.7072 (2)	0.1096 (1)	0.4299 (2)	4.24 (4)
Br(2)	0.3664 (2)	−0.1203 (1)	0.2720 (1)	3.45 (4)
Br(3)	0.5988 (2)	0.0170 (1)	0.1634 (1)	4.88 (5)
P(1)	0.3491 (4)	0.1055 (3)	0.2128 (3)	2.9 (1)
P(2)	0.6834 (4)	−0.1490 (3)	0.3604 (4)	3.3 (1)
C(10)	0.454 (1)	0.0363 (9)	0.479 (1)	2.3 (3)
C(11)	0.287 (2)	0.063 (1)	0.075 (1)	5.0 (5)
C(12)	0.178 (2)	0.115 (1)	0.004 (1)	6.7 (6)
C(13)	0.214 (1)	0.127 (1)	0.258 (1)	3.9 (4)
C(14)	0.133 (2)	0.048 (1)	0.259 (2)	5.0 (5)
C(15)	0.403 (2)	0.216 (1)	0.189 (1)	4.3 (5)
C(16)	0.447 (2)	0.273 (1)	0.294 (2)	4.5 (5)
C(21)	0.845 (2)	−0.131 (1)	0.439 (2)	5.8 (6)
C(22)	0.918 (2)	−0.074 (2)	0.388 (2)	6.7 (6)
C(23)	0.631 (2)	−0.242 (1)	0.432 (2)	4.9 (5)
C(24)	0.704 (2)	−0.328 (1)	0.445 (2)	6.7 (7)
C(25)	0.697 (2)	−0.203 (1)	0.235 (1)	5.0 (5)
C(26)	0.576 (2)	−0.232 (1)	0.155 (2)	6.5 (6)

[a] The equivalent isotropic displacement parameter, B_{eqv}, is calculated as $^1/_3[a^2a^{*2}B_{11} + b^2b^{*2}B_{22} + c^2c^{*2}B_{33} + 2ab(\cos\gamma)a^*b^*B_{12} + 2ac(\cos\beta)a^*c^*B_{13} + 2bc(\cos\alpha)b^*c^*B_{23}]$.

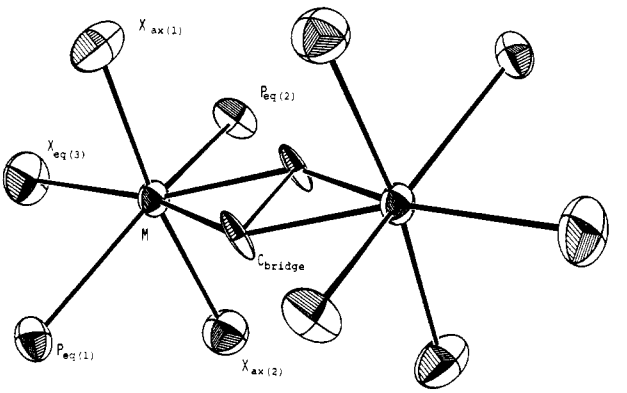

Figure 1. ORTEP drawing of a $M_2X_6(PEt_3)_4(CH_2CH_2)$ molecule with the atom-labeling scheme. The carbon atoms of the PEt_3 ligand are omitted for clarity. Atoms are represented by their ellipsoids at the 50% level.

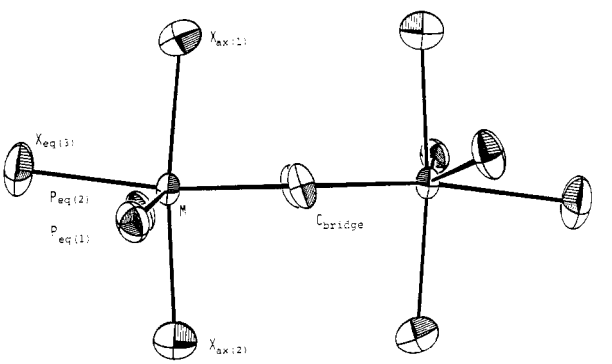

Figure 2. ORTEP drawing showing the side view of a $M_2X_6(PEt_3)_4(CH_2CH_2)$ molecule.

Results and Discussion

A generalized ORTEP drawing of the $M_2X_6(PR_3)_4(CH_2CH_2)$ structures is presented in Figure 1. Selected bond distances and angles for all compounds are listed in Table VI. Each $M_2X_6(PR_3)_4(CH_2CH_2)$ molecule resides on a crystallographic inversion center. While for each molecule the only rigorous symmetry is 1, each one has, effectively, the higher symmetry D_{2h}. All structures are essentially identical. A characteristic feature of

Table VI. Selected Bond Distances (Å) and Angles (deg) for $M_2X_6(PR_3)_4(CH_2CH_2)$

M	X	R	M–X_{eq}	M–X_{ax}	M–P_{eq}	M–C_b	C_b–C_b	C_b–M–C_b	X_{ax}–M–X_{ax}	P_{eq}–M–P_{eq}
Zr	Cl	Et	2.472 (5)	2.430 (6)	2.780 (5)	2.42 (2)	1.69 (3)	40.6 (6)	174.8 (2)	153.0 (2)
				2.428 (5)	2.793 (6)	2.44 (2)				
	Br	Et	2.629 (4)	2.597 (2)	2.798 (6)	2.41 (2)	1.56 (3)	37.9 (7)	172.0 (1)	150.0 (2)
				2.593 (3)	2.785 (6)	2.40 (2)				
Hf	Cl	Et	2.470 (3)	2.415 (3)	2.764 (3)	2.386 (10)	1.476 (14)	36.2 (3)	176.0 (1)	153.09 (9)
				2.410 (3)	2.773 (3)	2.364 (9)				
	Br	Et	2.619 (2)	2.589 (2)	2.775 (4)	2.36 (2)	1.51 (2)	37.1 (5)	173.08 (7)	150.2 (1)
				2.574 (2)	2.757 (5)	2.374 (15)				

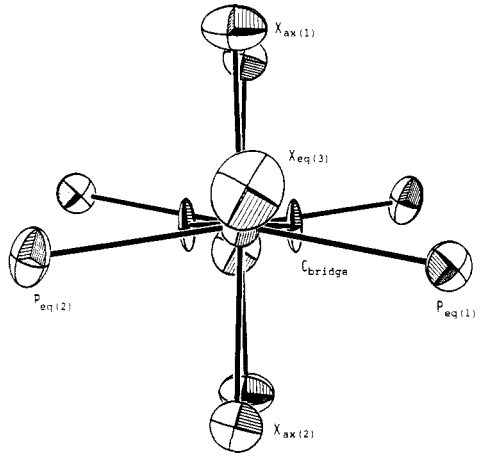

Figure 3. ORTEP drawing showing a $M_2X_6(PEt_3)_4(CH_2CH_2)$ molecule along the metal–metal axis.

these molecules is a symmetrical ethylene bridge in which the olefin plane is perpendicular to the metal–metal axis with the midpoint of the ethylene coinciding with the midpoint of the metal–metal vector. If we consider a line drawn from the midpoint of the ethylene toward each metal atom, then we could view the $M_2X_6(PR_3)_4(CH_2CH_2)$ molecule as a dimer consisting of two distorted octahedra, of trans,mer geometry, sharing the "ethylene corner". We define the nearly planar (see Figures 2 and 3) ten-atom arrangement consisting of the two metal atoms, the two bridging carbon atoms of the ethylene molecule, the four phosphorus nuclei, and two of the halide atoms as the equatorial plane. The structure is then completed with the four axial halide atoms, two above and two below the equatorial plane.

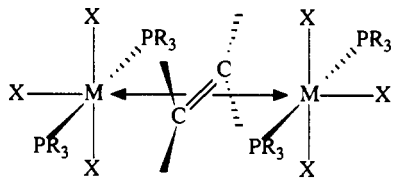

There are two main distortions from the octahedral geometry. The first is bending back of the four equatorial phosphine ligands away from the central $M_2(\mu\text{-}\eta^4\text{-olefin})$ unit by 27–30°. This distortion can be ascribed largely to steric repulsions between the alkyl groups of the phosphine ligands. Some distortion, although to smaller extent, must be caused by repulsion between the alkyl groups of the phosphine ligands and the hydrogen atoms of the ethylene bridge. The second distortion is less severe, about 4–8° (see Table VI) and represents bending of the axial halogen ligands toward the center of the molecule. The reasons for that distortion are unclear.

All metal to ligand distances are normal. The carbon–carbon bonds are rather long (>1.5 Å), which indicates that the C–C bond order has been reduced considerably but that a C–C bond of some importance still remains.

Our first observations were unplanned. We obtained **2** when attempting to employ 1,2-dichloroethane as a solvent for the bromo analogue of $Zr_2Cl_6(PEt_3)_4$.[4,5] We noted that the solution spontaneously and rapidly changed its color from green to orange. The red crystalline $Zr_2Br_6(PEt_3)_4(CH_2CH_2)$ (**2**) was isolated from the reaction mixture. We found that $Zr_2Cl_6(PEt_3)_4$ as well as the chloro and bromo hafnium analogues underwent similar reactions with 1,2-dichloroethane to give **1**, **3**, and **4**.

With the above structural results in hand we naturally wondered whether $M_2X_6(PR_3)_4$ species would react directly with ethylene to yield **1**–**4**. On reexamining ref 5a, we found that reactions of ethylene with $Zr_2Cl_6(PEt_3)_4$ had been already reported; however, no crystallographic work had been done and structures with Zr–C σ-bonds were proposed. This proposal of a σ-bonded structure seemed to be inspired by a previous report concerning $(Cp_2ZrX)_2C_2H_4$ compounds,[12] in which a very rough structure determination was used as the basis for suggesting the existence of two Zr–C σ-bonds. We obtained the compound originally formulated as $(Et_3P)_2Cl_3ZrCH_2CH_2ZrCl_3(PEt_3)_2$ in crystalline form, and we found it to be identical with our compound **1**. Hafnium analogues **3** and **4** were also synthesized by this alternative route by saturating the toluene solutions of the presumed $Hf_2X_6(PEt_3)_4$ species with ethylene.

The now available spectroscopic evidence ($^{31}P\{H\}$ NMR) suggests that at first one molecule of $M_2X_6(PR_3)_4$ reacts with 1,2-dichloroethane to give monomeric $MX_3Cl(PR_3)_2$ and ethylene.

$$M_2X_6(PR_3)_4 + 1,2\text{-}C_2H_4Cl_2 \rightarrow 2MX_3Cl(PR_3)_2 + CH_2CH_2 \quad (1)$$

The released ethylene reacts in turn with another molecule of $M_2X_6(PR_3)_4$ to give the title compounds.

$$M_2X_6(PR_3)_4 + CH_2CH_2 \rightarrow M_2X_6(PR_3)_4(CH_2CH_2) \quad (2)$$

We attempted to prepare $M_2X_6(PR_3)_4(CR'_2CR'_2)$ complexes in which one or more hydrogen atoms of the ethylene molecule would be substituted with alkyl groups. To that end we reacted $M_2X_6(PR_3)_4$ compounds (M = Zr, Hf; X = Cl, Br) with 1,2-dichloropropane, 3,4-dichlorobutane, propylene, *trans*- and *cis*-2-butene, 2,3-dimethyl-2-butene, and 1-butene. The reactions appeared to take place as evidenced by color change of the reaction mixtures. Unfortunately, we were unable to crystallize any solid products from those extremely air-sensitive solutions. After standing in a freezer for several days, the solutions turned colorless. Upon evaporation of the solvents only oily, polymeric, residues were obtained.

Very crude calculations and model building show that substituting even a single hydrogen atom of the ethylene bridge with a methyl group is obstructed by alkyl groups of the two phosphine ligands that are trans to each other. Therefore, we believe that, for steric reasons, it may be impossible to introduce substituted ethylene molecules as bridging ligands unless, of course, the phosphine ligands could be influenced to take a cis arrangement. We tried to react *cis,cis*-$Zr_2Cl_6(dppe)_2$, a molecule in which the chelating phosphine ligands should retain the cis,cis arrangement, with 1,2-dichloroethane. Not only did $Zr_2Cl_6(dppe)_2$ fail to react, but it was recrystallized from 1,2-dichloroethane to give solvated crystals that were used in the structure determination of $Zr_2Cl_6(dppe)_2{\cdot}2C_2H_4Cl_2{\cdot}1.5C_7H_8$.[5b] $Zr_2Cl_6(dppe)_2$ was also unreactive toward ethylene. The fact that an ethylene-bridged product was not obtained might suggest that the trans disposition of the phosphine ligands in $M_2X_6(PR_3)_4(CH_2CH_2)$ complexes is essential to stability. However, we cannot reconcile the difference

(12) (a) Sinn, H.; Kolk, E. *J. Organomet. Chem.* **1966**, *6*, 373. (b) Kaminsky, W.; Kopf, J.; Sinn, H.; Vollmer, H.-J. *Angew. Chem., Int. Ed. Engl.* **1976**, *15*, 629.

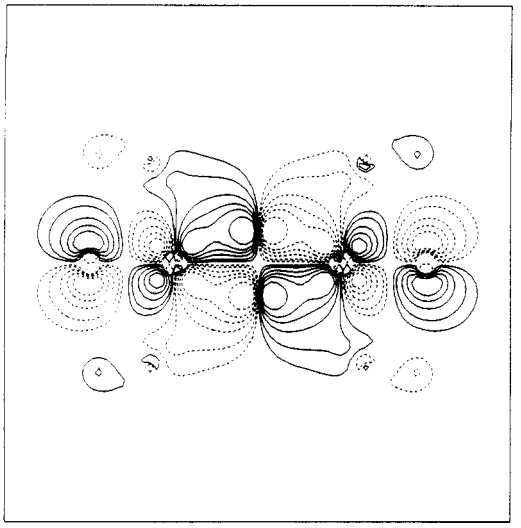

Figure 4. Contour plot of the $6b_{2g}$ molecular orbital (HOMO) of $Zr_2Cl_6(PH_3)_4(CH_2CH_2)$.

in the reactivity toward 1,2-dichloroethane of the starting materials that contain chelating phosphines compared to those that do not.

Having established structural features of $M_2X_6(PR_3)_4(CH_2CH_2)$ complexes, we directed our attention to the questions of bonding and electronic structure in the $M_2(\mu\text{-}\eta^4\text{-olefin})$ unit. As the first approximation we could view $M_2X_6(PR_3)_4(CH_2CH_2)$ as an example of a 4-center–4-electron bond. If we consider the molecule to be assembled from two $MX_3(PR_3)_2$ units and the $H_2C{=}CH_2$ molecule, we can envision two major contributions to the bonding. In the first one, $\Psi_{b_{1u}}$, the π orbital of CH_2CH_2

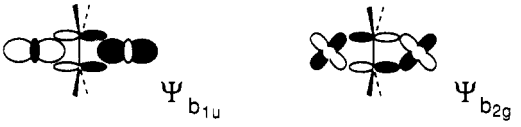

and its pair of electrons can interact with a pair of σ-type orbitals on the two metal atoms to give a bonding, occupied b_{1u} molecular orbital. Overlap between suitable $d\pi$ orbitals (or $d\pi$–$p\pi$ hybrids) on the metal atoms with the π^* orbital of CH_2CH_2 and the population of the resulting b_{2g} bonding orbital by two electrons (the unpaired electrons on the formally d^1, $MX_3(PR_3)_2$, units) should provide the second important contribution, $\Psi_{b_{2g}}$.

In order to determine the relative importance of these two contributions, the electronic structure of the $M_2X_6(PR_3)_4(CH_2CH_2)$ complexes was investigated by a molecular orbital calculation on the $Zr_2Cl_6(PH_3)_4(CH_2CH_2)$ model at the level of the Fenske–Hall approximation.

Calculations

The calculations on the $Zr_2Cl_6(PH_3)_4(CH_2CH_2)$ molecule result in a molecular orbital diagram with 47 doubly occupied valence molecular orbitals. Among the occupied MOs, there are 10 a_g type, 8 b_{1u} type, 7 b_{2u} and b_{3u} types, 6 b_{2g} type, 4 b_{3g} type, 3 b_{1g} type, and 2 a_u type. Because of the length of the table that lists these molecular orbitals together with their energies and percent characters, it is included in supplementary material rather than in this report. However, important features of the orbitals will be presented here and discussed. The calculations show that the b_{1u} contribution to the bonding, which arises from an interaction of the π orbital of CH_2CH_2 with a pair of σ-type orbitals on two Zr metal atoms, is spread over a number of b_{1u} MOs rather than being clearly identifiable in any one. However, the b_{2g} contribution resulting from an overlap between suitable $d\pi$ orbitals on the metal atoms with the π^* orbital of CH_2CH_2 is clearly identified as the HOMO (the combined metal and carbon character is 75.8%). The contour plot of this $6b_{2g}$ orbital (HOMO) is shown in Figure 4.

The calculations show a very large HOMO to LUMO gap of 5.93 eV. We are thus inclined to believe that analogues of $M_2X_6(PR_3)_4(CH_2CH_2)$ complexes in which there are more electrons, e.g. Nb and Ta analogues, may not be obtainable. That conclusion finds an experimental support in the work of Sattelberger and co-workers.[13] They reported that *cis,trans*-$Ta_2Cl_6(PMe_3)_4$ reacts readily and cleanly with CH_2CH_2 to give the monomeric tantalum(III)–ethylene complex *trans,mer*-$TaCl_3(PMe_3)_2(CH_2CH_2)$.

Acknowledgment. We thank the Robert A. Welch Foundation for support under Grant No. A494.

Supplementary Material Available: Full listings of crystal data, bond distances, bond angles, and isotropic equivalent displacement parameters for $Zr_2Cl_6(PEt_3)_4(CH_2CH_2)$ (**1**), $Zr_2Br_6(PEt_3)_4(CH_2CH_2)$ (**2**), $Hf_2Cl_6(PEt_3)_4(CH_2CH_2)$ (**3**), and $Hf_2Br_6(PEt_3)_4(CH_2CH_2)$ (**4**) and valence molecular orbitals, their energies, and percent characters for $Zr_2Cl_6(PH_3)_4(CH_2CH_2)$ (17 pages); tables of observed and calculated structure factors for **1**–**4** (36 pages). Ordering information is given on any current masthead page.

(13) Sattelberger, A. P.; Wilson, R. B., Jr.; Huffman, J. C. *J. Am. Chem. Soc.* **1980**, *102*, 7113.